

Effects of thermal motion on electromagnetically induced absorption

E. Tilchin and A. D. Wilson-Gordon

Department of Chemistry, Bar-Ilan University, Ramat Gan 52900, Israel

O. Firstenberg

Department of Physics, Technion-Israel Institute of Technology, Haifa 32000, Israel

We describe the effect of thermal motion and buffer-gas collisions on a four-level closed N system interacting with strong pump(s) and a weak probe. This is the simplest system that experiences electromagnetically induced absorption (EIA) due to transfer of coherence via spontaneous emission from the excited to ground state. We investigate the influence of Doppler broadening, velocity-changing collisions (VCC), and phase-changing collisions (PCC) with a buffer gas on the EIA spectrum of optically active atoms. In addition to exact expressions, we present an approximate solution for the probe absorption spectrum, which provides physical insight into the behavior of the EIA peak due to VCC, PCC, and wave-vector difference between the pump and probe beams. VCC are shown to produce a wide pedestal at the base of the EIA peak, which is scarcely affected by the pump-probe angular deviation, whereas the sharp central EIA peak becomes weaker and broader due to the residual Doppler-Dicke effect. Using diffusion-like equations for the atomic coherences and populations, we construct a spatial-frequency filter for a spatially structured probe beam and show that Ramsey narrowing of the EIA peak is obtained for beams of finite width.

PACS numbers: 42.50.Gy, 32.70.Jz

I. INTRODUCTION

The absorption spectrum of a weak probe, interacting with a pumped nearly-degenerate two-level transition, can exhibit either a sharp subnatural dip or peak at line center [1], depending on the degeneracy of the levels, the polarizations of the fields, and the absence or presence of a weak magnetic field. The phenomenon is termed electromagnetically-induced transparency (EIT) [2, 3] when there is a dip in the probe spectrum and electromagnetically induced absorption (EIA) [4] when there is a peak.

In the case of orthogonal polarizations of the pump and probe, both EIT and EIA are related to the ground-level Zeeman coherence, which is induced by the simultaneous action of both fields. The simplest model system that exhibits EIT is the three-level Λ system, where the two lower states $g_{1,2}$ are Zeeman sublevels of the ground hyperfine level F_g . In a Λ system, quantum coherence can lead to the destructive interference between the two possible paths of excitation. As a result, if the pump field is tuned to resonance, the narrow dip in the probe absorption spectrum at the two-photon resonance can be interpreted as EIT caused by a coherent population trapping [5] in the lower levels. The simplest system that exhibits EIA is the four-level N system [6, 7] (Fig. 1, top), consisting of states $g_{1,2}$ and $e_{1,2}$ which are Zeeman sublevels of the ground (F_g) and excited (F_e) hyperfine levels, where the $g_i \leftrightarrow e_i$, $i = 1, 2$, transitions interact with non-saturating pump(s), and the $g_2 \leftrightarrow e_1$ transition interacts with a weak probe. The N system gives similar results to those obtained for a closed alkali-metal $F_g \rightarrow F_e = F_g + 1$ transition interacting with a σ_{\pm} polarized pump, and a weak π polarized probe [7, 8]. It has been shown [6, 7, 9], that the EIA peak is due to

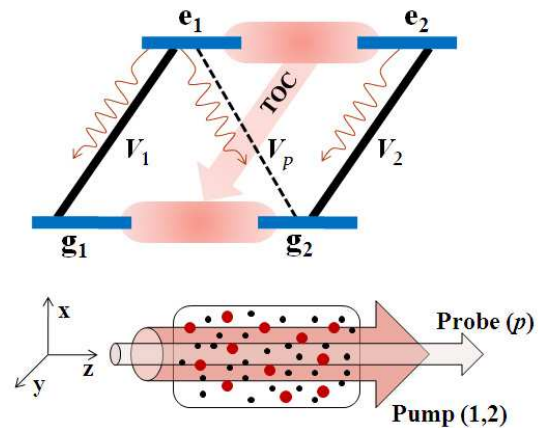


FIG. 1: Top: The N -configuration atom. The light-induced transitions are marked by solid (pump field) and dashed (probe field) lines, and the wavy arrows are spontaneous decay paths. The thick arrow illustrates the spontaneous transfer of coherence (TOC). Bottom: probe and pump beam(s), of possibly a finite size, propagating through the vapor cell. The optical axis is parallel to \hat{z} , while \hat{x} and \hat{y} form the optical transverse plane.

transfer of coherence (TOC) from the excited state to the ground state, via spontaneous emission. The excited-state coherence only exists in systems where the coherent population trapping is incomplete so that there is some population in the excited state [9, 10]. The transfer of this coherence to the ground state leads to a peak in the contribution of the ground-state two-photon coherence to the probe absorption at line center, instead of the dip that occurs in its absence (for example, in a Λ system or a non-degenerate N system) [11].

In this paper, we investigate the effect of the thermal motion of the alkali-metal gas on the EIA spectrum, in the presence of a buffer gas. In a previous paper [12], we discussed the effect of phase-changing collisions (PCC) with the buffer gas on an N system and showed that they lead to considerable narrowing of the EIA peak in both the presence and absence of Doppler broadening. These collisions increase the transverse decay rate of the optical transitions, resulting in the so-called pressure broadening of the optical spectral line, and are thus easily incorporated in the Bloch equations. However, in order to describe the overall effect of buffer-gas collisions, it is necessary to include both velocity-changing collisions (VCC) as well as PCC [13, 14], which is a much greater challenge. Due to the complexity of the problem, we limit our discussion to a four-level N system, and to buffer-gas pressures that are sufficiently low so that collisional decoherence of the excited state [15] can be neglected.

The Doppler effect occurs in the limit of *ballistic* atomic motion, when the mean free-path between VCC is much larger than the radiation wavelength. Due to their narrow spectral response, Raman processes such as EIT and EIA are much more sensitive to the “residual” Doppler effect, arising when there is a difference between the wavevectors of the Raman fields. In many cases however, the Raman wavelength can become much larger than the typical free-path between collisions. For example, an angular deviation of a milliradian between the two optical beams yields a superposition pattern with a wavelength in the order of a millimeter. In this limit, the atoms effectively perform a *diffusion* motion through the spatial oscillations of the superposition field, leading to the Dicke narrowing of the residual Doppler width. While the residual Doppler broadening is linearly proportional to the Raman wavevector, Dicke narrowing shows a quadratic dependence. This behavior was demonstrated in EIT with non-collimated pump and probe [16, 17].

Recently, a model describing thermal motion and collisions for EIT was presented [17–19], utilizing the density matrix distribution in space and velocity with a Boltzmann relaxation formalism. The model describes a range of motional phenomena, including Dicke narrowing, and diffusion in the presence of electromagnetic fields and during storage of light. This diffusion model was used to describe a spatial frequency filter for a spatially structured probe [19] and also Ramsey narrowing [20, 21]. Here, we utilize a similar formalism to estimate the influence of the atomic thermal motion in a buffer-gas environment, including VCC and PCC, on the spectral shape of EIA in a four-level N system, with collimated or non-collimated light beams. In Sec. II, the Doppler broadening and Dicke narrowing effects are studied for plane-wave fields. As the full mathematical treatment is lengthy, it appears in Appendix A. However, an approximate equation which describes the main features of the spectra is presented in Sec. II. Diffusion-like equations for the ground and excited state coherences and populations are derived in Appendix B. Two main phenomena

are described using this model: (i) a spatial-frequency filter for structured probe fields which is presented in Sec. III, and (ii) atomic diffusion through a finite-sized beam resulting in Ramsey narrowing of the EIA peak, which is discussed in Sec. IV. Finally, conclusions are drawn in Sec. V.

II. THE DOPPLER-DICKE LINE SHAPES OF EIA

Consider the near-resonant interaction of a four-state atom in an N configuration, depicted in Fig. 1. The two lower states g_1 and g_2 are degenerate and belong to the ground level with zero energy, and the excited states e_1 and e_2 are degenerate with energy $\hbar\omega_0$. The light field consists of three beams, each with a carrier frequency ω_j and wavevector \mathbf{q}_j , where $j = 1, 2$ denotes the two strong pump beams, and $j = p$ the weak probe,

$$\check{\mathbf{E}}(\mathbf{r}, t) = \sum_{j=1,2,p} \mathbf{E}_j(\mathbf{r}, t) e^{-i\omega_j t + i\mathbf{q}_j \cdot \mathbf{r}} + \text{c.c.} \quad (1)$$

Here, $\mathbf{E}_j(\mathbf{r}, t)$ are the slowly varying envelopes in space and time. The pumps drive the $g_1 \leftrightarrow e_1$ and $g_2 \leftrightarrow e_2$ transitions, and the probe is coupled to the $g_2 \leftrightarrow e_1$ transition.

Our model will incorporate four relaxation rates: Γ , the spontaneous emission rate from the each of the excited states to all the ground states; Γ_{pcc} , the pressure broadening of the optical transitions resulting from PCC; γ_{vcc} , the velocity autocorrelation relaxation rate ($1/\gamma_{\text{vcc}}$ is the time it takes the velocity vector to vary substantially) [22], which is proportional to the rate of VCC; and γ is the homogenous decoherence rate within the ground and excited state manifolds due, for example, to spin-exchange and spin-destruction collisions [26]. In the model, the transition $g_1 \leftrightarrow e_2$ is forbidden (due to some selection rule such as angular momentum).

To focus the discussion, we assume that all three beams are continuous waves, namely $\mathbf{E}_j(\mathbf{r}, t) = \mathbf{E}_j(\mathbf{r})$. We then obtain stationary Rabi frequencies, given by $V_j = V_j(\mathbf{r}) = \mu_j \mathbf{E}_j(\mathbf{r})/\hbar$, where μ_j is the transition dipole moment. The complete set of Bloch equations for the four-level N system consists of sixteen equations [7]. In order to simplify the application of the theory to EIA, we assume that $V_p \ll V_{1,2} < \Gamma$ and that the pump transitions are well below saturation, so that in the absence of the probe, the population concentrates in the g_2 state, the $g_2 \leftrightarrow e_2$ dipole is excited, and the e_2 state is empty up to second order in the pump field [7]. The equations can then be written up to the first order in the probe field V_p [6], which reduces the number of Bloch equations to five.

The complete analytical development is presented in Appendix A, and an example of the calculated probe absorption spectrum for collinear and degenerate beams ($\mathbf{q}_1 = \mathbf{q}_2 = \mathbf{q}$) is given in Fig. 2(a) (blue line). For the

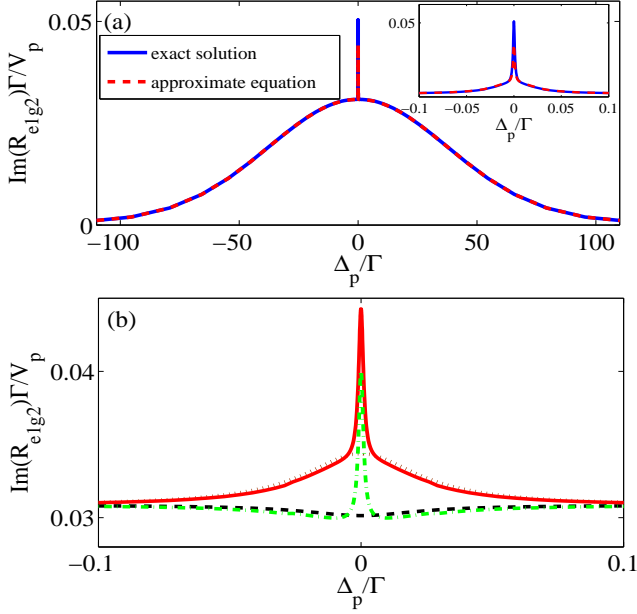


FIG. 2: (a) The probe absorption, calculated from the exact solution for the density matrix (blue line) and from the approximate solution Eq. (7) (red line), for collinear plane-wave beams ($\mathbf{q}_1 = \mathbf{q}_2 = \mathbf{q}_p$), $\Gamma_{\text{pcc}} = 5\Gamma$, $\gamma_{\text{vcc}} = 0.025\Gamma$, $A = 0.816$, $V_2 = 0.1\Gamma$, $V_1 = AV_2$, $V_p = \gamma = 0.001\Gamma$, and $\Delta_1 = \Delta_2 = 0$. The inset depicts a zoom on the EIA peak with its wide pedestal. (b) The EIA spectrum (red line) is the sum of three contributions in Eq. (7): the one-photon absorption (black dashed line), a pedestal at the base of the peak (brown dotted line), and the sharp peak (green dash-dotted line). For the clarity of presentation, the one-photon absorption is added to the pedestal and to the sharp peak curves.

numerical calculations, we have considered the D_2 line of ^{85}Rb (wavelength 780 nm) at room temperature, with a total spontaneous emission rate $\Gamma = 2\pi \times 6$ MHz [23]. Other parameters are indicated in the figure caption and described in what follows.

Four complex frequencies control the EIA dynamics, each relating to a different coherence in the process:

$$\xi_1 = (\Delta_p - \Delta_1) - (\mathbf{q}_p - \mathbf{q}_1) \cdot \mathbf{v} + i(\gamma + \gamma_{\text{vcc}}), \quad (2a)$$

$$\xi_2 = \Delta_p - \mathbf{q}_p \cdot \mathbf{v} + i(\tilde{\Gamma} + \gamma_{\text{vcc}}), \quad (2b)$$

$$\xi_3 = (\Delta_p - \Delta_2) - (\mathbf{q}_p - \mathbf{q}_2) \cdot \mathbf{v} + i(\Gamma + \gamma + \gamma_{\text{vcc}}), \quad (2c)$$

$$\xi_4 = (\Delta_p - \Delta_1 - \Delta_2) - (\mathbf{q}_p - \mathbf{q}_1 - \mathbf{q}_2) \cdot \mathbf{v} + i(\tilde{\Gamma} + \gamma_{\text{vcc}}), \quad (2d)$$

with the one-photon detunings $\Delta_j = \omega_j - \omega_{e_j g_j}$ ($j = 1, 2$) and $\Delta_p = \omega_p - \omega_{e_1 g_2}$, and $\tilde{\Gamma} = \Gamma/2 + \Gamma_{\text{pcc}} + \gamma$. The frequency ξ_2 is related to the probe transition and includes the one-photon Doppler shift $\mathbf{q}_p \cdot \mathbf{v}$. ξ_1 and ξ_3 relate to the slowly varying ground and excited state coherences and include the residual Doppler shift $(\mathbf{q}_p - \mathbf{q}_i) \cdot \mathbf{v}$ and the

Raman (two-photon) detuning. ξ_4 relates to the three-photon transition (whose direct optical-dipole is forbidden), required for the EIA process. Note that the fast optical decay rates (Γ or $\tilde{\Gamma}$) is absent only from ξ_1 .

In EIA, in contrast to EIT, a strong optical-dipole transition ($g_2 \leftrightarrow e_2$) is excited even in the absence of the probe. Its excitation depends on its resonance with the pump field, and is thus affected by Doppler broadening. This leads to velocity-dependent equations even in zero-order in the probe field, and introduces the additional complex frequency

$$\xi_5 = -\Delta_2 + \mathbf{q}_2 \cdot \mathbf{v} + i(\tilde{\Gamma} + \gamma_{\text{vcc}}), \quad (3)$$

with the one-photon Doppler shift $\mathbf{q}_2 \cdot \mathbf{v}$. The overall dynamics is thus governed by the five equations (A9a)-(A9e).

We start by calculating the probe absorption spectrum for uniform pump and probe fields (plane waves) by solving the equations analytically. The spectrum depends on 18 different integrals over velocity, of the form

$$G_i = \int d^3v \frac{\xi_\alpha \cdots \xi_\beta}{\xi_5 \xi_d} F(\mathbf{v}), \quad (4)$$

where $F(\mathbf{v}) = (2\pi v_{\text{th}}^2)^{-3/2} e^{-\mathbf{v}^2/2v_{\text{th}}^2}$ is the Boltzmann velocity distribution, and $v_{\text{th}}^2 = k_b T/m$ is the mean thermal velocity. The determinant ξ_d ,

$$\xi_d = \xi_1 \xi_2 \xi_3 \xi_4 - \xi_3 (\xi_2 V_2^2 + \xi_4 V_1^2) + iV_1 V_2 b A \Gamma (\xi_2 + \xi_4), \quad (5)$$

introduces the power broadening effect (first and second terms), *i.e.* the dependence of the Raman spectral width on the pump powers, and the spontaneous TOC from the excited state to the ground state (last term). The last term is associated with the TOC due to its dependence on the parameter b , which sets the amount of TOC in the original dynamic equations (A1), and can take either the value 0 (no TOC) or 1 [6]. The spontaneous decay branching ratio is given by $A^2 = \mu_{e_1 g_1}^2 / (\mu_{e_1 g_1}^2 + \mu_{e_1 g_2}^2)$ [7]. The TOC term in Eq. (5) depends on the complex frequency

$$\xi_2 + \xi_4 = (2\Delta_p - \Delta_1 - \Delta_2) - (2\mathbf{q}_p - \mathbf{q}_1 - \mathbf{q}_2) \cdot \mathbf{v} + 2i(\Gamma/2 + \Gamma_{\text{pcc}} + \gamma + \gamma_{\text{vcc}}). \quad (6)$$

It is important to note that, although each of the individual frequencies ξ_2 and ξ_4 is affected by a Doppler shift (either one- or three-photon), the sum $\xi_2 + \xi_4$ exhibits *only a residual Doppler shift* (assuming nearly collinear pumps, $\mathbf{q}_1 \approx \mathbf{q}_2$). Nevertheless the relaxation rate $(\Gamma/2 + \Gamma_{\text{pcc}} + \gamma + \gamma_{\text{vcc}})$ is the same as that characterizing the decay of the optical transitions. As a consequence, even when Γ_{pcc} is much smaller than the optical Doppler width, it plays a significant role in determining the intensity of the EIA spectrum. This is in contrast to one- and two-photon processes (such as EIT), in which Γ_{pcc}

is irrelevant when it is much smaller than the Doppler width. It can also be seen that when $\mathbf{q}_1 \approx \mathbf{q}_2$, the various residual Doppler shifts are negligible compared to the relaxation rates in the determinant ξ_d , so that ξ_d is only weakly dependent on these shifts.

Examining the absorption spectrum in Fig. 2(a), we observe the narrow absorption peak on top of the broad one-photon curve. Moreover, as can be seen in the inset, the EIA resonance consists of two independent features: a “pedestal” at the base and a sharp absorption peak at the center. In order to obtain physical insight into these features, we have derived an approximate solution for the probe absorption which incorporates the main contributions to the EIA, namely the underlying EIT mechanism plus the spontaneous TOC. The approximate Fourier transform of the nondiagonal density-matrix element for the probe is

$$R_{e_1 g_2} = n_0 \left[-G_4 + V_2^2 G_5 + iV_1 V_2 b A \Gamma \frac{iG_2 G_3 \gamma_{\text{vcc}}}{1 - iG_1 \gamma_{\text{vcc}}} \right] V_p, \quad (7)$$

where $G_1 = \int d^3 v \frac{\xi_2 \xi_3 \xi_4 F(\mathbf{v})}{\xi_d}$, $G_2 = \int d^3 v \frac{\xi_3 \xi_4 F(\mathbf{v})}{\xi_d}$, $G_3 = \int d^3 v \frac{\xi_2 \xi_4 F(\mathbf{v})}{\xi_5 \xi_d}$, $G_4 = \int d^3 v \frac{\xi_1 \xi_3 \xi_4 F(\mathbf{v})}{\xi_d}$, $G_5 = \int d^3 v \frac{\xi_3 F(\mathbf{v})}{\xi_d}$, and n_0 is the number density of the active atoms. It can be shown that Eq. (7) is valid provided $\gamma_{\text{vcc}} \ll \Gamma_{\text{pcc}} + \Gamma/2$. For an atom at rest and in the absence of collisions, so that $\gamma_{\text{vcc}} = 0$, $v_{\text{th}} \rightarrow 0$, and $\Gamma_{\text{pcc}} = 0$, Eq. (7) is identical to the expression obtained by Taichenachev *et al.* [6] (with $b = 1$),

$$R_{e_1 g_2}^{\text{rest}} = \frac{in_0 V_p}{\Gamma/2 - i\Delta_p} \left[1 + \frac{2A |V_1|^2 / \Gamma}{2(1 - A^2) |V_2|^2 / \Gamma - i\Delta_p} \right]. \quad (8)$$

The first term in the square brackets in Eqs. (7) and (8) describes the one-photon (background) absorption, and the other terms are the EIA peak.

For a moving atom, the spectrum resulting from Eq. (7) is shown in Fig. 2(a) (red dashed line) and is compared with the exact solution; evidently, there is a good agreement between the spectra. Despite the small discrepancy in the intensity of the sharp peak, the approximate solution preserves the main features in the resonance. When plotted separately in Fig. 2(b), the three terms in Eq. (7) can be identified with the different spectral features: $-G_4$ (black dashed line) describes the background absorption; $V_2^2 G_5$ (brown dotted line), which constitutes the total peak in the absence of VCC, describes the wide pedestal; and $iG_2 G_3 \gamma_{\text{vcc}} / (1 - G_1 \gamma_{\text{vcc}})$ (green dashed-dotted line) describes the sharp EIA peak, induced by VCC.

Fig. 3 shows the effect of varying the VCC rate, for a fixed PCC rate ($\Gamma_{\text{pcc}} = 5\Gamma$) and zero pump-probe angular deviation. The width of the pedestal feature depends on the VCC rate and is given by $\gamma_{\text{vcc}} + \gamma$, while the width of the narrow peak shows only a very weak dependence on γ_{vcc} . Increasing the VCC rate leads to a decrease in the overall EIA intensity, but to an increase in the

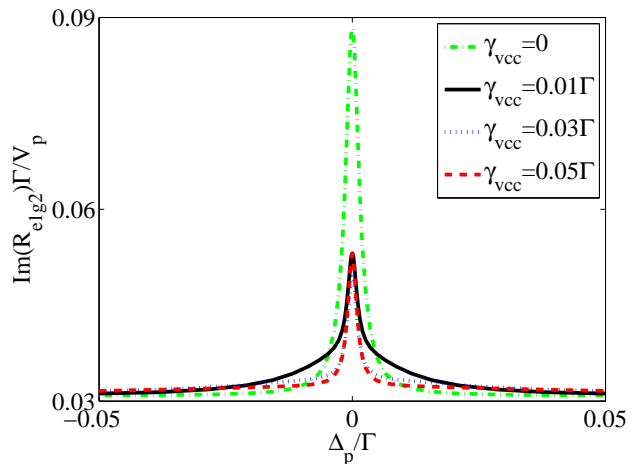


FIG. 3: The EIA peak for different γ_{vcc} rates and $\Gamma_{\text{pcc}} = 5\Gamma$ at zero pump-probe angular deviation; other parameters as in Fig. 2

ratio between the amplitude of the narrow peak and the pedestal baseline.

We now turn to explore the residual (two-photon and four-photon) Doppler and Dicke effects due to wave-vector mismatch between the pump fields and the probe, introduced in principle either by a frequency detuning between the fields, $|\mathbf{q}_p| \neq |\mathbf{q}_{1,2}|$, or due to an angular deviation between them, $\mathbf{q}_p \not\parallel \mathbf{q}_{1,2}$. We mainly focus on the latter, which may be found in a nearly degenerate level scheme, and we further take the two pump fields to be the same, namely $\mathbf{q}_1 = \mathbf{q}_2$. Figure 4 presents the probe absorption spectrum for different values of the wave-vector difference, $\delta\mathbf{q} = \mathbf{q}_p - \mathbf{q}_{1,2}$, when $\gamma_{\text{vcc}} = 0.1\Gamma$ and $\Gamma_{\text{pcc}} = \Gamma$. As can be seen, increasing $\delta\mathbf{q}$ broadens the EIA spectrum (see inset). This is analogous to the broadening of an EIT transmission peak in a similar configuration [17]. However, the wide collisionally-broadened pedestal remains unaffected by the changes in $\delta\mathbf{q}$, indicating that it mostly originates from homogenous decay processes. Figure 5(a) summarizes the full-width at half-maximum (FWHM) of the EIA peak for $\Gamma_{\text{pcc}} = \Gamma$ and for various values of γ_{vcc} , as a function of $\delta\mathbf{q}$. Because of the difficulty of separating the sharp peak from the background in the calculated spectra [27], the widths of the sharp EIA peak were obtained only from the third term in Eq. (7). In contrast to an EIT peak, which does not depend on γ_{vcc} when $\delta\mathbf{q} = \mathbf{0}$ (collinear degenerate beams) [19], the FWHM of the EIA peak at $\delta\mathbf{q} = \mathbf{0}$ depends weakly on the VCC rate (although barely noticeable in the figure). This difference derives from the effect of collisions on the pump absorption in the case of EIA, as described earlier.

For $\delta\mathbf{q} \neq \mathbf{0}$ the FWHM of the peak in the Dicke limit (high γ_{vcc}) depends on γ_{vcc} and is proportional to the residual Doppler-Dicke width, $2v_{\text{th}}\delta\mathbf{q}^2/\gamma_{\text{vcc}}$. In this limit,

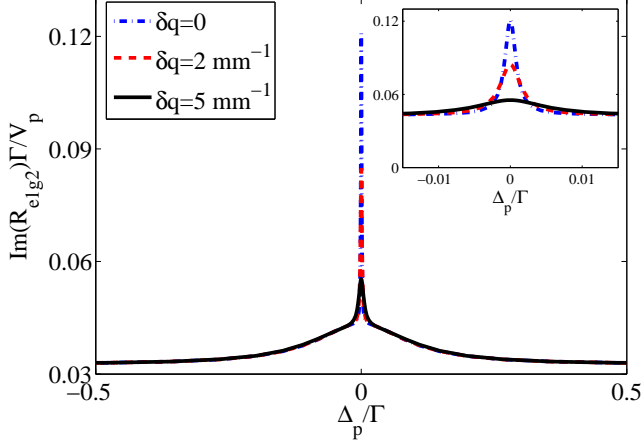


FIG. 4: Calculated probe absorption spectra with $\gamma_{\text{vcc}} = 0.1\Gamma$ and $\Gamma_{\text{pcc}} = \Gamma$, for different pump-probe angular deviations. Other parameters as in Fig. 2.

the results are well approximated by the analytic expression [19] [dotted lines in Fig. 5(a)]:

$$\text{FWHM} = 2 \times \frac{2}{a^2} \gamma_{\text{vcc}} H\left(a \frac{v_{\text{th}} \delta q}{\gamma_{\text{vcc}}}\right), \quad (9)$$

where $H(x) = e^{-x} - 1 + x$ and $a^2 = 2/\ln 2$. Increasing the pump-probe angular deviation reduces the efficiency of the EIA process and thus results in a decrease in the probe absorption [Fig. 5(b)]. This is of course the opposite trend to that of EIT (blue stars), where the depth of the dip decreases (the absorption increases) with increasing δq [19].

III. SPATIAL-FREQUENCY FILTER

We now turn to discuss the results of our model from the viewpoint of a spatial-frequency filter for a structured probe beam. When non-uniform beams are considered, the different spatial frequencies that comprise the beams result in different Doppler and Dicke widths. Consequently, the various spatial-frequency components experience different absorption and refraction in the medium. Specifically, the dependence of the absorption on the transverse wave-vectors of the probe beam manifests a filter for the probe in Fourier space.

We assume an optical configuration of two collinear uniform pumps (plane waves with V_1 and V_2 constant) and a spatially varying propagating probe, $V_p = V_p(\mathbf{r}, t)$. Since the medium exhibits a non-local response due to the atomic motion, the evolution of the probe is more naturally described in the Fourier space $V_p(\mathbf{k}, \omega)$ where \mathbf{k} and ω are the spatial and temporal frequencies of the envelope of the probe. Under these assumptions, the model results in a Diffusion-like equations for the populations and

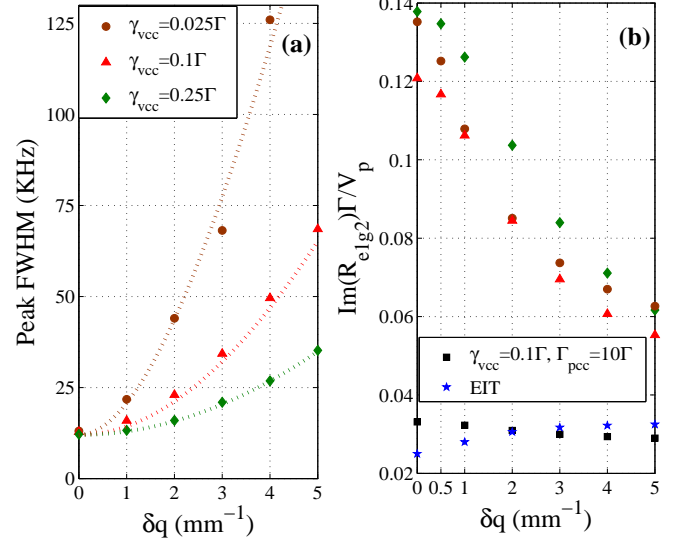


FIG. 5: Calculated EIA FWHM (a) and absorption (b) for $\Gamma_{\text{pcc}} = \Gamma$ and various values of γ_{vcc} , as a function of the pump-probe wave-vector difference $\delta \mathbf{q}$. The blue stars are the EIT absorption on the Raman resonance conditions, with $\Gamma_{\text{pcc}} = \Gamma$ and $\gamma_{\text{vcc}} = 0.025\Gamma$.

coherences of the atomic medium, derived in Appendix B. To simplify the general dynamics of Eqs. (B8a) and (B9), we take the stationary case [$\omega = 0$, $V_p = V_p(\mathbf{k})$] and assume that the carrier wave-vector of the probe is the same as that of the pumps, $\mathbf{q}_p = \mathbf{q}_1 = \mathbf{q}_2$, so that $\delta \mathbf{q}_1 = \delta \mathbf{q}_2 = 0$. Taking the Fourier transform [see Eq. (A11)], we obtain a set of steady-state equations for the spatially-dependent atomic coherences, $R_{g_1 g_2}(\mathbf{k})$, $R_{e_1 e_2}(\mathbf{k})$, and $R_{e_1 g_2}(\mathbf{k})$,

$$\begin{aligned} & \left[i(\Delta_p - \Delta_1) - \gamma - K_{1p} |V_1|^2 - K_{3p} |V_2|^2 - Dk^2 \right] R_{g_1 g_2} \\ & = (Dk^2 - bA\Gamma) R_{e_1 e_2} + K_{1p} V_1^* V_p n_0, \end{aligned} \quad (10a)$$

$$\begin{aligned} & \left[i(\Delta_p - \Delta_2) - \Gamma - \gamma - Dk^2 \right] R_{e_1 e_2} \\ & = -V_1 V_2^* (K_{1p} + K_{3p}) R_{g_1 g_2} - V_2^* (K_{1p} + K_{\text{pump}}) V_p n_0, \end{aligned} \quad (10b)$$

$$R_{e_1 g_2} = iK_{1p} (V_1 R_{g_1 g_2} + V_p n_0) \quad (10c)$$

where $K_{1p} = iG_{1p}/(1 - iG_{1p}\gamma_{\text{vcc}})$ is the one-photon absorption spectrum with $G_{1p} = \int F(\mathbf{v})/\xi_2 d^3v$; $K_{3p} = iG_{3p}/(1 - iG_{3p}\gamma_{\text{vcc}})$ is the three-photon absorption spectrum with $G_{3p} = \int F(\mathbf{v})/\xi_4 d^3v$; and $K_{\text{pump}} = iG_{\text{pump}}/(1 - iG_{\text{pump}}\gamma_{\text{vcc}})$ is the one-photon (pump) absorption spectrum with $G_{\text{pump}} = \int F(\mathbf{v})/\xi_5 d^3\mathbf{v}$, as described in Appendix B. Solving Eq. (10) for $R_{e_1 g_2}(\mathbf{k}, \omega)$, substituting the result into the expression for the linear-susceptibility [Eq. (A14)], assuming that $V_1 = \eta V_2$ ($0 < \eta \leq 1$), and neglecting all the terms proportional to $1/\Gamma$, we obtain

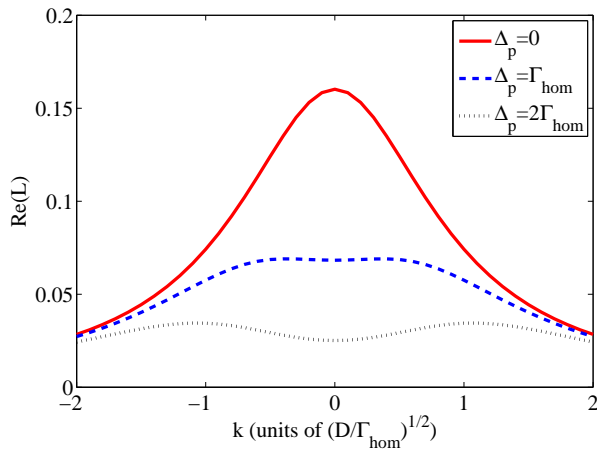


FIG. 6: The EIA spatial-frequency filter, given in Eq. (11b), as a function of k , with $\gamma_{\text{vcc}} = 0.025\Gamma$ and $\Gamma_{\text{pcc}} = 10\Gamma$. Red curve is plotted for Δ_p on resonance, blue-dashed and black-dotted curves demonstrate the behavior at nonzero Raman detuning.

$$\chi_{e_1 g_2}(\mathbf{k}) = \frac{g}{c} i K n_0 (1 + L), \quad (11a)$$

$$L = \frac{\eta(2bA - \eta)\Gamma_p}{-i\Delta_p + \gamma + (\eta^2 + 1 - 2bA\eta)\Gamma_p + Dk^2}, \quad (11b)$$

where $D = v_{th}/\gamma_{\text{vcc}}$ is the diffusion coefficient, $\Gamma_p = K|V_2|^2$ is the power broadening, and $K_{1p} \approx K_{3p} \approx K_{\text{pump}} = K = \int F(\mathbf{v}) / [\mathbf{q}_p \cdot \mathbf{v} + i(\Gamma/2 + \Gamma_{\text{pcc}} + \gamma + \gamma_{\text{vcc}})] d^3v$ for $\Delta_p \ll \Gamma_{\text{hom}} = \gamma + \Gamma_p$. In the case where $\eta = A$, Eqs. (11) is similar to Eq. (8) obtained by Taichenachev *et al.* [6], except for the diffusion term Dk^2 , which vanishes for an atom at rest.

The imaginary part of the susceptibility in Eq. (11) yields the absorption of the probe for various values of \mathbf{k} . The first term in the brackets in Eq. (11a) is the linear one-photon absorption, and the second term is the k -dependent EIA contribution. Thus, the real part of L in Eq. (11b) describes an ‘‘absorbing’’ spatial-frequency filter, the same way as was done for EIT [24, 25]. Fig. 6 summarizes several examples of the EIA spatial filter behavior as a function of k for $\Delta_p = 0$, $\Delta_p = \pm\Gamma_{\text{hom}}$, and $\Delta_p = \pm 2\Gamma_{\text{hom}}$. At $\Delta_p = 0$, the curve is a Lorentzian and maximum absorption is achieved. When $\Delta_p \neq 0$ the filter becomes more transparent.

IV. RAMSEY NARROWING

We now consider the N system interacting with collinear probe and pump beams that have finite widths. Due to thermal motion, the alkali atoms spend a period

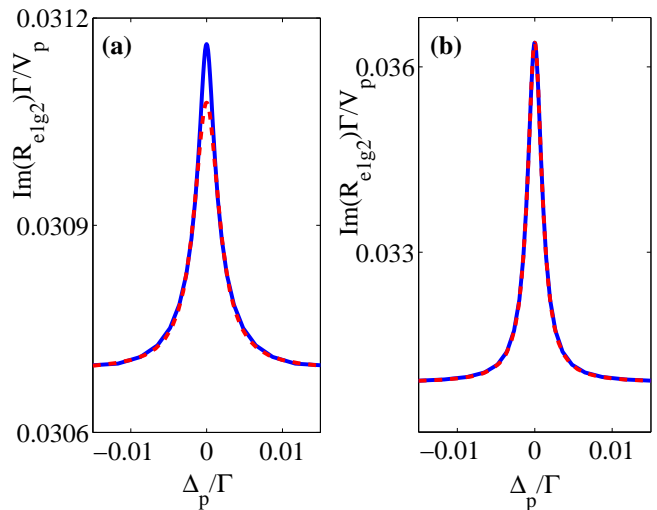


FIG. 7: Calculated probe absorption spectra (blue line) for one-dimensional stepwise beam with finite thickness: (a) $2a = 100 \mu\text{m}$ and (b) $2a = 10 \text{mm}$, and fitted Lorentzian (red dashed line). All other parameters are the same as in Fig. 2

of time in the interaction region and then leave the light beams, evolve ‘in the dark’, and diffuse back inside. Such a random periodic motion was described recently by Xiao *et al.* [20, 21] for an EIT system, and was shown to result in a cusp-like spectrum. Near its center, the line is much narrower than that expected from time-of-flight broadening and power broadening, and the effect, resulting from the contribution of bright-dark-bright atomic trajectories of random durations, was named Ramsey narrowing.

Ramsey-narrowed spectra can be calculated analytically from the diffusion equations of the atomic coherences when the light fields of both the probe and pump beams have finite widths [19]. The EIA spectrum resulting from a one-dimensional uniform light-sheet of thickness $2a$ in the x -direction is derived analytically in Appendix B [Eq. (B12)]. In Fig. 7, we show the spectrum for two different thicknesses and the fitted Lorentzian curves. Near the resonance, the EIA line for the $100 \mu\text{m}$ sheet is spectrally sharper than the fitted Lorentzian – the characteristic signature of Ramsey narrowing. In contrast, the EIA peak calculated for a 10mm beam is well fitted by the Lorentzian. In addition, the EIA contrast deteriorates as the beam becomes narrower, since the interaction area decreases and fewer atoms interact with the fields.

V. CONCLUSIONS

In this paper, we extended the theory that describes the effect of buffer-gas collisions on three-level Λ systems in an EIT configuration [17–19] to the case of a four-level closed N system which is the simplest system that

experiences EIA due to TOC. Using this formalism, we investigated the influence of collisions of optically active atoms with a buffer gas on the EIA peak. In addition to the exact expressions, we presented an approximate solution for the probe absorption spectrum, which provides a physical insight into the behavior of the EIA peak due to VCC, PCC, and wave-vector difference between the pump and probe beams. VCC were shown to produce a wide pedestal at the base of the EIA peak; increasing the pump-probe angular deviation scarcely affects the pedestal whereas the sharp central EIA peak becomes weaker and broader due to the residual Doppler-Dicke effect. Using diffusion-like equations for the atomic coherences and populations, the spatial-frequency filter and the Ramsey-narrowed spectrum were analytically obtained.

In extending the description from the Λ to the N schemes, we have considered several elements that are likely to be important in other four-level systems. These include the diffusion of excited-state coherences and the influence of the thermal motion on the optical dipole in the absence of the probe. The latter introduces a Doppler contribution into the pumping terms and consequently affects the power broadening of the narrow resonances.

Appendix A: Reduced density matrix

Consider the near-resonant interaction of a light field consisting of one or two moderately strong pumps and a weak probe, as given in Eq. (1), with the four-level degenerate N system of Fig. 1(a). We use the first-order approximation in the probe amplitude, V_p , and assume that $V_2 < \Gamma$, $V_1 \leq V_2$, $V_p < V_{1,2}$. Since the pump transitions are assumed non-saturated, the atomic population in the absence of the probe concentrates in the g_2 state, and the population in other states can be neglected. The $g_2 \leftrightarrow e_2$ dipole, excited in the absence of the probe, is of importance and is thus considered. The resulting Bloch equations are [6]

$$\begin{aligned} \dot{\rho}_{g_1 g_2}^{(1),i}(\omega_p - \omega_1) &= -[i(\omega_{e_1 g_2} - \omega_{e_1 g_1}) + \gamma] \check{\rho}_{g_1 g_1}^{(1),i} \\ &+ i\check{V}_1^* \check{\rho}_{e_1 g_2}^{(1),i} - i\check{V}_2 \check{\rho}_{g_1 e_2}^{(1),i} + bA\Gamma \check{\rho}_{e_1 e_2}^{(1),i}, \end{aligned} \quad (\text{A1a})$$

$$\begin{aligned} \dot{\rho}_{e_1 g_2}^{(1),i}(\omega_p) &= -[i\omega_{e_1 g_2} + \Gamma/2 + \Gamma_{\text{pcc}}] \check{\rho}_{e_1 g_2}^{(1),i} \\ &+ i\check{V}_p \check{\rho}_{g_2 e_2}^{(0),i} + i\check{V}_1 \check{\rho}_{g_1 e_2}^{(1),i}, \end{aligned} \quad (\text{A1b})$$

$$\begin{aligned} \dot{\rho}_{e_1 e_2}^{(1),i}(\omega_p - \omega_2) &= -[i(\omega_{e_1 g_2} - \omega_{e_2 g_2}) + \Gamma + \gamma] \check{\rho}_{e_1 e_2}^{(1),i} \\ &+ i\check{V}_p \check{\rho}_{g_2 e_2}^{(0),i} + i\check{V}_1 \check{\rho}_{g_1 e_2}^{(1),i} - i\check{V}_2^* \check{\rho}_{e_1 g_2}^{(1),i}, \end{aligned} \quad (\text{A1c})$$

$$\begin{aligned} \dot{\rho}_{g_1 e_2}^{(1),i}(\omega_p - \omega_1 - \omega_2) &= -[i(\omega_{e_1 g_2} - \omega_{e_1 g_1} - \omega_{e_2 g_2}) \\ &+ \Gamma/2 + \Gamma_{\text{pcc}}] \check{\rho}_{g_1 g_1}^{(1),i} - i\check{V}_2^* \check{\rho}_{g_1 g_2}^{(1),i}, \end{aligned} \quad (\text{A1d})$$

$$\begin{aligned} \dot{\rho}_{g_2 e_2}^{(0),i}(-\omega_2) &= -[\Gamma/2 + \Gamma_{\text{pcc}} - i\omega_{e_2 g_2}] \check{\rho}_{g_2 e_2}^{(0),i}(-\omega_2) \\ &+ i\check{V}_2^* \left(\check{\rho}_{e_2 e_2}^{(0),i} - \check{\rho}_{g_2 g_2}^{(0),i} \right). \end{aligned} \quad (\text{A1e})$$

Here, $\check{\rho}_{ss'}^{(j),i}$ is the density-matrix element of the i -th atom (one of many identical particles) to the j -th order in the probe, and apart from $\check{\rho}_{g_2 g_2}^{(0),i} \approx 1$, $\check{\rho}_{ss}^{(0),i} = 0$. We also consider the envelopes of the pumps to be constant in time so that $V_{1,2}$ is shorthand for $V_{1,2}(\mathbf{r})$. The wave equation for the probe field is

$$\left(\nabla^2 - \frac{1}{c^2} \frac{\partial^2}{\partial t^2} \right) \check{\mathbf{E}}_p(\mathbf{r}, t) = \frac{4\pi}{c^2} \frac{\partial^2}{\partial t^2} \check{\mathbf{P}}_{e_1 g_2}(\mathbf{r}, t), \quad (\text{A2})$$

where $\check{\mathbf{P}}_{e_1 g_2}(\mathbf{r}, t) = \mathbf{P}_{e_1 g_2}(\mathbf{r}, t) e^{-i\omega_p t} e^{-i\mathbf{q}_p \cdot \mathbf{r}}$ is the contribution of the $e_1 \leftrightarrow g_2$ transition to the expectation value of the polarization, $\mathbf{P}_{e_1 g_2}$ is the slowly varying polarization, and ∇^2 is the three-dimensional Laplacian operator. With Eq. (1), and assuming without loss of generality that $\hat{\mathbf{q}}_p = \hat{\mathbf{z}}q_p$, as shown in Fig. 1(b), Eq. (A2) can be written in the paraxial approximation as

$$\left(\frac{\partial}{\partial t} + c \frac{\partial}{\partial z} - i \frac{c}{2q_p} \nabla_{\perp}^2 \right) V_p(\mathbf{r}, t) = i \frac{g}{\mu_{e_1 g_2}^*} \mathbf{P}_{e_1 g_2}(\mathbf{r}, t), \quad (\text{A3})$$

where ∇_{\perp}^2 is the transverse Laplacian operator, and $g = 2\pi\omega_p |\mu_{e_1 g_2}|^2 / \hbar$ is a coupling constant.

Following [19], we introduce a density-matrix distribution function in space and velocity,

$$\check{\rho}_{ss'} = \check{\rho}_{ss'}(\mathbf{r}, \mathbf{v}, t) = \sum_i \check{\rho}_{ss'}^i(t) \delta(\mathbf{r} - \mathbf{r}_i(t)) \delta(\mathbf{v} - \mathbf{v}_i(t)), \quad (\text{A4})$$

where the time dependence of $\check{\rho}_{ss'}^i(t)$ is determined by Eqs. (A1). Differentiating Eq. (A4) with respect to time, we arrive at

$$\begin{aligned} \frac{\partial}{\partial t} \check{\rho}_{ss'} + \mathbf{v} \cdot \frac{\partial}{\partial \mathbf{r}} \check{\rho}_{ss'} + \left[\frac{\partial}{\partial t} \check{\rho}_{ss'} \right]_{\text{col}} \\ = \sum_i \frac{\partial}{\partial t} \check{\rho}_{ss'}^i(t) \delta(\mathbf{r} - \mathbf{r}_i(t)) \delta(\mathbf{v} - \mathbf{v}_i(t)), \end{aligned} \quad (\text{A5})$$

where the effect of velocity-changing collisions is taken in the strong collision limit in the form of a Boltzmann relaxation term [22],

$$\left[\frac{\partial}{\partial t} \check{\rho}_{ss'} \right]_{\text{col}} = -\gamma_{\text{vcc}} \left[\check{\rho}_{ss'}(\mathbf{r}, \mathbf{v}, t) - \check{R}_{ss'}(\mathbf{r}, t) F(\mathbf{v}) \right], \quad (\text{A6})$$

with $\check{R}_{ss'} = \check{R}_{ss'}(\mathbf{r}, t) = \int d^3\mathbf{v} \check{\rho}_{ss'}(\mathbf{r}, \mathbf{v}, t)$ being the density-number of atoms per unit volume, near \mathbf{r} in space, and

$$F = F(\mathbf{v}) = (2\pi v_{\text{th}})^{-3/2} e^{-\mathbf{v}^2/2v_{\text{th}}^2}, \quad v_{\text{th}} = \frac{k_b T}{m} \quad (\text{A7})$$

is the Boltzmann distribution.

Before writing the coupled dynamics of the internal and motional degrees of freedom, we introduce the slowly

varying envelopes of the density-matrix elements, $\rho_{ss'} = \rho_{ss'}(\mathbf{r}, \mathbf{v}, t)$, as

$$\begin{aligned}\check{\rho}_{g_1g_2} &= \rho_{g_1g_2} e^{-i(\omega_p - \omega_1)t} e^{i(\mathbf{q}_p - \mathbf{q}_1) \cdot \mathbf{r}}, \\ \check{\rho}_{e_1g_2} &= \rho_{e_1g_2} e^{-i\omega_p t} e^{i\mathbf{q}_p \cdot \mathbf{r}}, \\ \check{\rho}_{e_1e_2} &= \rho_{e_1e_2} e^{i(\mathbf{q}_p - \mathbf{q}_2) \cdot \mathbf{r}}, \\ \check{\rho}_{g_1e_2} &= \rho_{g_1e_2} e^{-i(\omega_p - \omega_1 - \omega_2)t} e^{i(\mathbf{q}_p - \mathbf{q}_1 - \mathbf{q}_2) \cdot \mathbf{r}}, \\ \check{\rho}_{g_2e_2} &= \rho_{g_2e_2} e^{i\omega_2 t} e^{-i\mathbf{q}_2 \cdot \mathbf{r}},\end{aligned}\quad (\text{A8})$$

and similarly the slowly varying densities $R_{ss'} = \int d^3\mathbf{v} \rho_{ss'}$. Eqs. (A1) then become

$$\begin{aligned}\left[\frac{\partial}{\partial t} + \mathbf{v} \cdot \frac{\partial}{\partial \mathbf{r}} - i\xi_1 \right] \rho_{g_1g_2} - \gamma_{\text{vcc}} R_{g_1g_2} F \\ = i(V_1^* \rho_{e_1g_2} - V_2 \rho_{g_1e_2}) + bA\Gamma \rho_{e_1e_2},\end{aligned}\quad (\text{A9a})$$

$$\begin{aligned}\left[\frac{\partial}{\partial t} + \mathbf{v} \cdot \frac{\partial}{\partial \mathbf{r}} - i\xi_2 \right] \rho_{e_1g_2} - \gamma_{\text{vcc}} R_{e_1g_2} F \\ = i[V_p n_0 F + V_1 \rho_{g_1g_2}],\end{aligned}\quad (\text{A9b})$$

$$\begin{aligned}\left[\frac{\partial}{\partial t} + \mathbf{v} \cdot \frac{\partial}{\partial \mathbf{r}} - i\xi_3 \right] \rho_{e_1e_2} - \gamma_{\text{vcc}} R_{e_1e_2} F \\ = i(V_1 \rho_{g_1e_2} - V_2^* \rho_{e_1g_2}) + iV_p \rho_{g_2e_2},\end{aligned}\quad (\text{A9c})$$

$$\begin{aligned}\left[\frac{\partial}{\partial t} + \mathbf{v} \cdot \frac{\partial}{\partial \mathbf{r}} - i\xi_4 \right] \rho_{g_1e_2} - \gamma_{\text{vcc}} R_{g_1e_2} F \\ = -iV_2^* \rho_{g_1g_2},\end{aligned}\quad (\text{A9d})$$

$$\begin{aligned}\left[\frac{\partial}{\partial t} + \mathbf{v} \cdot \frac{\partial}{\partial \mathbf{r}} - i\xi_5 \right] \rho_{g_2e_2} - \gamma_{\text{vcc}} R_{g_2e_2} F \\ = -iV_2^* n_0 F,\end{aligned}\quad (\text{A9e})$$

where ξ_i ($i = 1 - 5$) are given in Eq. (2). The expectation value of the polarization density $\mathbf{P}_{e_1g_2}(\mathbf{r}, t)$ in terms of the number density $R_{e_1g_2}(\mathbf{r}, t)$ is $\mathbf{P}_{e_1g_2}(\mathbf{r}, t) = \mu_{e_1g_2}^* R_{e_1g_2}(\mathbf{r}, t)$, and Eq. (A3) becomes

$$\left(\frac{\partial}{\partial t} + c \frac{\partial}{\partial z} - i \frac{c}{2q_p} \nabla_{\perp}^2 \right) V_p(\mathbf{r}, t) = ig R_{e_1g_2}(\mathbf{r}, t).\quad (\text{A10})$$

We now consider the case of stationary plane-wave pumps. For this case, it is convenient to introduce the Fourier transform

$$f(\mathbf{r}, t) = \int_{-\infty}^{+\infty} \frac{d^3k}{2\pi} e^{i\mathbf{k}\mathbf{r}} \int_{-\infty}^{+\infty} \frac{d\omega}{2\pi} e^{-i\omega t} f(\mathbf{k}, \omega),\quad (\text{A11})$$

and write Eqs. (A9) as

$$\begin{aligned}[\omega - \mathbf{k} \cdot \mathbf{v} + \xi_1] \rho_{g_1g_2} - i\gamma_{\text{vcc}} R_{g_1g_2}(\mathbf{k}, \omega) F \\ = (V_2 \rho_{g_1e_2} - V_1^* \rho_{e_1g_2}) + ibA\Gamma \rho_{e_1e_2},\end{aligned}\quad (\text{A12a})$$

$$\begin{aligned}[\omega - \mathbf{k} \cdot \mathbf{v} + \xi_2] \rho_{e_1g_2} - i\gamma_{\text{vcc}} R_{e_1g_2}(\mathbf{k}, \omega) F \\ = -(V_p n_0 F + V_1 \rho_{g_1g_2}),\end{aligned}\quad (\text{A12b})$$

$$\begin{aligned}[\omega - \mathbf{k} \cdot \mathbf{v} + \xi_3] \rho_{e_1e_2} - i\gamma_{\text{vcc}} R_{e_1e_2}(\mathbf{k}, \omega) F \\ = (V_2^* \rho_{e_1g_2} - V_1 \rho_{g_1e_2}) - V_p \rho_{g_2e_2},\end{aligned}\quad (\text{A12c})$$

$$\begin{aligned}[\omega - \mathbf{k} \cdot \mathbf{v} + \xi_4] \rho_{g_1e_2} - i\gamma_{\text{vcc}} R_{g_1e_2}(\mathbf{k}, \omega) F \\ = V_2^* \rho_{g_1g_2},\end{aligned}\quad (\text{A12d})$$

$$\begin{aligned}[\omega - \mathbf{k} \cdot \mathbf{v} + \xi_5] \rho_{g_2e_2} - i\gamma_{\text{vcc}} R_{g_2e_2}(\mathbf{k}, \omega) F \\ = V_2^* n_0 F,\end{aligned}\quad (\text{A12e})$$

and Eq. (A10) as

$$\left(ik_z - \frac{i\omega}{c} + i \frac{k^2}{2q_p} \right) V_p(\mathbf{k}, \omega) = i \frac{g}{c} R_{e_1g_2}(\mathbf{k}, \omega).\quad (\text{A13})$$

The linear susceptibility $\chi_{e_1g_2}(\mathbf{k}, \omega)$ is defined by

$$R_{e_1g_2}(\mathbf{k}, \omega) = \chi_{e_1g_2}(\mathbf{k}, \omega) \frac{c}{g} V_p(\mathbf{k}, \omega).\quad (\text{A14})$$

In order to find the probe absorption spectrum, we solve Eqs. (A12) analytically, obtain an expression for $\rho_{ss'}$, and formally integrate it over velocity. This leads to an expression for $R_{ss'}$ in terms of integrals over velocity, in the form of Eq. (4), such as $G_1 = \int d^3v \frac{\xi_2 \xi_3 \xi_4 F(\mathbf{v})}{\xi_d}$, which can be evaluated numerically. In the general case, the resulting expression for $R_{ss'}$ is very complicated and is not reproduced here. In order to explore the underlying physics, we developed an approximate expression for the Fourier transform of the density-matrix element that refers to the probe transition, namely, $R_{e_1g_2}$ [see Eq. (7)].

One can verify that in the absence of the pumps ($V_1 = V_2 = 0$), the resulting one-photon complex spectrum simplifies to the well known result for the strong collision regime, $K = iG/(1 - i\gamma_{\text{vcc}}G)$, where $G = \int d^3\mathbf{v} F/(\omega - \mathbf{k} \cdot \mathbf{v} + \xi_2)$ [22].

Appendix B: Diffusion in the presence of fields

In order to obtain diffusion-like equations for the density-matrix elements and the probe fields, we begin by integrating Eqs. (A9a) and (A9c) over velocity and obtain

$$\left[\frac{\partial}{\partial \mathbf{r}} + i\delta \mathbf{q}_1 \right] \cdot \mathbf{J}_{g_1 g_2} + \left[\frac{\partial}{\partial t} - i(\Delta_p - \Delta_1) + \gamma \right] R_{g_1 g_2} = i(V_1^* R_{e_1 g_2} - V_2 R_{g_1 e_2}) + bA\Gamma R_{e_1 e_2}, \quad (\text{B1a})$$

$$\left[\frac{\partial}{\partial \mathbf{r}} + i\delta \mathbf{q}_2 \right] \cdot \mathbf{J}_{e_1 e_2} + \left[\frac{\partial}{\partial t} - i(\Delta_p - \Delta_2) + \Gamma + \gamma \right] R_{e_1 e_2} = i(V_1 R_{g_1 e_2} - V_2^* R_{e_1 g_2} + V_p R_{g_2 e_2}), \quad (\text{B1b})$$

where $\mathbf{J}_{ss'} = \mathbf{J}_{ss'}(\mathbf{r}, t) = \int d^3 v \mathbf{v} \rho_{ss'}$ is the envelope of the current density. Expanding $\rho_{g_1 g_2}$ and $\rho_{e_1 e_2}$ in Eqs. (A9a) and (A9c) as $\rho_{ss'} = R_{ss'} F + 1/\gamma_{\text{vcc}} \rho_{ss'}^{(1)}$, multiplying Eqs. (A9a) and (A9c) by \mathbf{v} , integrating the resulting equations over velocity using

$$\int d^3 v_j v_i \frac{\partial}{\partial x_i} R_{ss'} F = \delta_{ij} v_{\text{th}} \frac{\partial}{\partial x_i} R_{ss'}, \quad (\text{B2})$$

defining the current density of the density matrix by

$$\gamma_{\text{vcc}} \mathbf{J}_{ss'} = \int d^3 v_j \rho_{ss'}^{(1)}, \quad (\text{B3})$$

and retaining the leading terms in $1/\gamma_{\text{vcc}}$, we obtain

$$\mathbf{J}_{g_1 g_2} + D \left[\frac{\partial}{\partial \mathbf{r}} + i\delta \mathbf{q}_1 \right] R_{g_1 g_2} = \frac{i}{\gamma_{\text{vcc}}} (V_1^* \mathbf{J}_{e_1 g_2} - V_2 \mathbf{J}_{g_1 e_2}) - \frac{bA\Gamma}{\gamma_{\text{vcc}}} \mathbf{J}_{e_1 e_2}, \quad (\text{B4a})$$

$$\mathbf{J}_{e_1 e_2} + D \left[\frac{\partial}{\partial \mathbf{r}} + i\delta \mathbf{q}_2 \right] R_{e_1 e_2} = \frac{i}{\gamma_{\text{vcc}}} (V_1 \mathbf{J}_{g_1 e_2} - V_2^* \mathbf{J}_{e_1 g_2} + \tilde{V}_p \mathbf{J}_{g_2 e_2}), \quad (\text{B4b})$$

where $D = v_{\text{th}}/\gamma_{\text{vcc}}$. Substituting $\mathbf{J}_{g_1 g_2}$, $\mathbf{J}_{e_1 e_2}$ from Eq. (B4) into Eq. (B1), we get

$$\left[\frac{\partial}{\partial t} - i(\Delta_p - \Delta_1) + \gamma - D \left(\frac{\partial}{\partial \mathbf{r}} + i\delta \mathbf{q}_1 \right)^2 \right] R_{g_1 g_2} = i(V_1^* R_{e_1 g_2} - V_2 R_{g_1 e_2}) + bA\Gamma R_{e_1 e_2} - D \left(\frac{\partial}{\partial \mathbf{r}} + i\delta \mathbf{q}_1 \right)$$

$$\times \left[\frac{i}{\gamma_{\text{vcc}}} (V_1^* \mathbf{J}_{e_1 g_2} - V_2 \mathbf{J}_{g_1 e_2}) - \frac{bA\Gamma}{\gamma_{\text{vcc}}} \mathbf{J}_{e_1 e_2} \right], \quad (\text{B5a})$$

$$\left[\frac{\partial}{\partial t} - i(\Delta_p - \Delta_2) + \Gamma + \gamma - D \left(\frac{\partial}{\partial \mathbf{r}} + i\delta \mathbf{q}_2 \right)^2 \right] R_{e_1 e_2} = i(V_1 R_{g_1 e_2} - V_2^* R_{e_1 g_2} + V_p R_{g_2 e_2}) - D \left(\frac{\partial}{\partial \mathbf{r}} + i\delta \mathbf{q}_2 \right)$$

$$\times \left[\frac{i}{\gamma_{\text{vcc}}} (V_1 \mathbf{J}_{g_1 e_2} - V_2^* \mathbf{J}_{e_1 g_2} + V_p \mathbf{J}_{g_2 e_2}) \right]. \quad (\text{B5b})$$

In order to calculate $R_{e_1 g_2}$, $R_{g_1 e_2}$, $R_{g_2 e_2}$, and $\mathbf{J}_{e_1 g_2}$, $\mathbf{J}_{g_1 e_2}$, $\mathbf{J}_{g_2 e_2}$, we assume in Eqs. (A9b), (A9d), and (A9e) that the envelopes change slowly enough such that $|\partial/\partial t + \mathbf{v} \cdot \partial/\partial \mathbf{r}| \ll |\xi_{2,4,5}|$, and get

$$-i\xi_2 \rho_{e_1 g_2} = \gamma_{\text{vcc}} R_{e_1 g_2} F + i(V_p n_0 F + V_1 \rho_{g_1 g_2}), \quad (\text{B6a})$$

$$-i\xi_4 \rho_{g_1 e_2} = \gamma_{\text{vcc}} R_{g_1 e_2} F - iV_2^* \rho_{g_1 g_2}, \quad (\text{B6b})$$

$$-i\xi_5 \rho_{g_2 e_2} = \gamma_{\text{vcc}} R_{g_2 e_2} F - iV_2^* n_0 F. \quad (\text{B6c})$$

Solving Eq. (B6) formally for $\rho_{e_1 g_2}$, $\rho_{g_1 e_2}$, $\rho_{g_2 e_2}$ and substituting only their leading parts, *i.e.* $\rho_{ss'} = R_{ss'} F$, we find

$$\rho_{e_1 g_2} = [\gamma_{\text{vcc}} R_{e_1 g_2} - V_1 R_{g_1 g_2}] - V_p n_0 F / \xi_2, \quad (\text{B7a})$$

$$\rho_{g_1 e_2} = [\gamma_{\text{vcc}} R_{g_1 e_2} + V_2^* R_{g_1 g_2}] F / \xi_4, \quad (\text{B7b})$$

$$\rho_{g_2 e_2} = [\gamma_{\text{vcc}} R_{g_2 e_2} + V_2^* n_0] F / \xi_5. \quad (\text{B7c})$$

Integrating Eqs. (B7) over velocity we get

$$R_{e_1 g_2} = iK_{1p} [V_1 R_{g_1 g_2} + V_p n_0], \quad (\text{B8a})$$

$$R_{g_1 e_2} = -iK_{3p} V_2^* R_{g_1 g_2}, \quad (\text{B8b})$$

$$R_{g_2 e_2} = -iK_{\text{pump}} V_2^* n_0, \quad (\text{B8c})$$

where $K_{1p} = iG_{1p}/(1 - G_{1p}\gamma_{\text{vcc}})$ is the one-photon absorption spectrum with $G_{1p} = \int F/\xi_2 d^3 v$, $K_{3p} = iG_{3p}/(1 - G_{3p}\gamma_{\text{vcc}})$ is the three-photon absorption spectrum with $G_{3p} = \int F/\xi_4 d^3 v$ and $K_{\text{pump}} = iG_{\text{pump}}/(1 - G_{\text{pump}}\gamma_{\text{vcc}})$ is the one-photon (pump) absorption spectrum with $G_{\text{pump}} = \int F/\xi_5 d^3 \mathbf{v}$. In the case of collinear pump and probe beams $\delta \mathbf{q} = \delta \mathbf{q}_{1,2} = \mathbf{q}_p - \mathbf{q}_{1,2} = \delta q \hat{\mathbf{z}}$, Eqs. (B5) and (B8) form a closed set when

$$\left(\frac{\partial}{\partial \mathbf{r}} + i\delta \mathbf{q}_{1,2} \right) \cdot \frac{iV_{1,2}(\mathbf{r})}{\gamma_{\text{vcc}}} \mathbf{J}_{e_1 g_2},$$

$$\left(\frac{\partial}{\partial \mathbf{r}} + i\delta \mathbf{q}_{1,2} \right) \cdot \frac{iV_{1,2}(\mathbf{r})}{\gamma_{\text{vcc}}} \mathbf{J}_{g_1 e_2},$$

$$\left(\frac{\partial}{\partial \mathbf{r}} + i\delta \mathbf{q}_2 \right) \cdot \frac{iV_p(\mathbf{r}, t)}{\gamma_{\text{vcc}}} \mathbf{J}_{g_2 e_2}$$

can be neglected in Eq. (B5). These terms vanish completely in the special case of pump and probe which are plane waves ($\partial/\partial \mathbf{r} = \mathbf{0}$), and also collinear and degenerate ($\delta \mathbf{q} = \mathbf{0}$). They can also be neglected whenever $|V_{1,2,p}| \ll \gamma_{\text{vcc}}$ as is the case in many realistic situations. However, the term $(\partial/\partial \mathbf{r} + i\delta \mathbf{q}_1) \cdot bA\Gamma/\gamma_{\text{vcc}} \mathbf{J}_{e_1 e_2}$ in Eq. (B5a) cannot be neglected in the case of collinear pump and probe beams since $bA\Gamma/\gamma_{\text{vcc}}$ does not go to zero.

Substituting Eq. (B4b) into Eq. (B5a), and Eq. (B8) into Eq. (B5), we find:

$$\begin{aligned}
& \left\{ \frac{\partial}{\partial t} - i(\Delta_p - \Delta_1) + \gamma + K_{1p} |V_1|^2 + K_{3p} |V_2|^2 \right\} R_{g_1 g_2} \\
& = D \left(\frac{\partial}{\partial \mathbf{r}} + i\delta \mathbf{q}_1 \right)^2 R_{g_1 g_2} + D \left(\frac{\partial}{\partial \mathbf{r}} + i\delta \mathbf{q}_2 \right)^2 R_{e_1 e_2} \\
& + bA\Gamma R_{e_1 e_2} - K_{1p} V_1^* V_p n_0, \tag{B9a} \\
& \left\{ \frac{\partial}{\partial t} - i(\Delta_p - \Delta_2) + \Gamma + \gamma \right\} R_{e_1 e_2} \\
& = D \left(\frac{\partial}{\partial \mathbf{r}} + i\delta \mathbf{q}_2 \right)^2 R_{e_1 e_2} + V_1 V_2^* (K_{1p} + K_{3p}) R_{g_1 g_2} \\
& + V_2^* (K_{1p} + K_{\text{pump}}) V_p n_0. \tag{B9b}
\end{aligned}$$

These are the final diffusion-like coupled equations for the ground- and excited-state coherences.

In order to investigate the Ramsey narrowing of the EIA peak, we consider finite probe and pump beams and restrict the discussion to collinear EIA. We assume that the fields are stationary and overlap in their cross sections with negligible variation along the z -direction, $V_p(\mathbf{r}, t) = V_p w(\mathbf{r}_\perp)$, $V_1(\mathbf{r}) = V_1 w(\mathbf{r}_\perp)$, $V_2(\mathbf{r}, t) = V_2 w(\mathbf{r}_\perp)$, where $w(\mathbf{r}_\perp)$ is the transverse profile of the fields. We further take $\delta q = 0$ and $\Delta_1 = \Delta_2 = 0$ for brevity. In the diffusion regime, we rewrite Eqs. (B8) and (B9) as

$$\begin{aligned}
& \left[i\Delta_p + \gamma + (K_{1p} |V_1|^2 + K_{3p} |V_2|^2) w(\mathbf{r}_\perp)^2 \right] R_{g_1 g_2} = \\
& bA\Gamma \left(1 + \frac{D}{\gamma_{\text{vcc}}} \nabla_\perp^2 \right) R_{e_1 e_2} - K_{1p} V_1^* V_p n_0 w(\mathbf{r}_\perp)^2, \tag{B10a}
\end{aligned}$$

$$R_{e_1 g_2} = iK_{1p} (V_1 R_{g_1 g_2} + V_p n_0) w(\mathbf{r}_\perp), \tag{B10b}$$

$$\begin{aligned}
& (i\Delta_p + \Gamma + \gamma - D\nabla_\perp^2) R_{e_1 e_2} \\
& = V_1 (K_{1p} + K_{3p}) R_{g_1 g_2} V_2^* w(\mathbf{r}_\perp)^2 \\
& + V_p (K_{1p} + K_{\text{pump}}) n_0 V_2^* w(\mathbf{r}_\perp)^2, \tag{B10c}
\end{aligned}$$

$$R_{g_1 e_2} = -iK_{3p} V_2^* R_{g_1 g_2} w(\mathbf{r}_\perp), \tag{B10d}$$

$$R_{g_1 e_2} = -iK_{\text{pump}} V_2^* n_0 w(\mathbf{r}_\perp). \tag{B10e}$$

We further consider a probe and pump beams with a uniform intensity and phase within a sheet of thickness $2a$ in the x -direction (one-dimensional stepwise beams):

$$w(x, y) = \begin{cases} 1 & \text{for } |x| \leq a \\ 0 & \text{for } |x| > a \end{cases}.$$

The solution for $R_{g_1 g_2}$, symmetric in x and decaying as $|x| \rightarrow \infty$, is given by

$$\begin{aligned}
& R_{g_1 g_2} (|x| \leq a) = \\
& C_2 \cosh(k_1 x) + C_1 \cosh(k_2 x) + \frac{bA\Gamma\beta_2 + D\alpha_2^2\beta_1}{(D\alpha_1\alpha_2)^2 + bA\Gamma\beta_3}, \tag{B11a}
\end{aligned}$$

$$\begin{aligned}
& R_{e_1 e_2} (|x| \leq a) = \frac{C_1 (k_2^2 - \alpha_2^2) D\gamma_{\text{vcc}}}{bA\Gamma (D\alpha_2^2 + \gamma_{\text{vcc}})} \cosh(k_2 x) \\
& + \frac{C_2 (k_1^2 - \alpha_1^2) D\gamma_{\text{vcc}}}{bA\Gamma (D\alpha_2^2 + \gamma_{\text{vcc}})} \cosh(k_1 x) + \frac{\beta_1\beta_3 - \beta_2\alpha_1^2 D}{\beta_3 bA\Gamma - (D\alpha_1\alpha_2)^2}, \tag{B11b}
\end{aligned}$$

$$\begin{aligned}
& R_{g_1 g_2} (|x| > a) = \\
& \frac{C_3 bA\Gamma (D\alpha_2^2 + \gamma_{\text{vcc}})}{(\alpha_3^2 - \alpha_2^2) D\gamma_{\text{vcc}}} e^{-\alpha_2(|x|-a)} + C_4 e^{-\alpha_3(|x|-a)}, \tag{B11c}
\end{aligned}$$

$$R_{e_1 e_2} (|x| > a) = C_3 e^{-\alpha_2(|x|-a)}, \tag{B11d}$$

where $\alpha_1^2 = (-i\Delta_p + \gamma + K_{1p} |V_1|^2 + K_{3p} |V_2|^2)/D$, $\alpha_2^2 = \alpha_3^2 + \Gamma/D$, $\alpha_3^2 = (-i\Delta_p + \gamma)/D$, and $\beta_1 = V_1^* V_p K_{1p} n_0$, $\beta_2 = V_1 V_2^* (K_{1p} + K_{3p})$, $\beta_3 = V_2^* V_p (K_{1p} + K_{\text{pump}}) n_0$. The complex diffusion wave-numbers are obtained from

$$\begin{aligned}
& 2D\gamma_{\text{vcc}} k_{1,2}^2 = D\gamma_{\text{vcc}} \alpha_\pm^2 + \beta_3 bA\Gamma \\
& \mp [(D\gamma_{\text{vcc}})^2 \alpha_\pm^4 + \beta_3 bA\Gamma (4 + 2D\gamma_{\text{vcc}} \alpha_\pm^2 + \beta_3 bA\Gamma)]^{1/2},
\end{aligned}$$

with $\alpha_\pm^2 = \alpha_2^2 \pm \alpha_1^2$. The coefficients C_i ($i = 1 - 4$) are obtained from the continuity conditions of $R_{ss'}$ and $(\partial/\partial x) R_{ss'}$ at $|x| = a$. From Eq. (B10b) one finds

$$\begin{aligned}
& R_{e_1 g_2} (|x| \leq a) = iK_2 \left[V_1 (C_2 \cosh(k_1 x) \right. \\
& \left. + C_1 \cosh(k_2 x) + \frac{bA\Gamma\beta_2 + D\alpha_2^2\beta_1}{(D\alpha_1\alpha_2)^2 + bA\Gamma\beta_3} \right) + V_p n_0 \right], \tag{B12}
\end{aligned}$$

and the energy absorption at frequency ω_p is finally calculated from $P(\Delta) = (\hbar\omega_p/a) \text{Im} \int_{-a}^a dx R_{e_1 g_2}(x)$. Two examples for the resulting spectrum are given in Fig. 7.

-
- [1] G. Khitrova, P. R. Berman, and M. Sargent, J. Opt. Soc. B **5**, 160 (1988).
[2] S. E. Harris, Phys. Today **50**, 36 (1997).
[3] M. Fleischhauer, A. Imamoglu, and J. P. Marangos, Rev. Mod. Phys. **77**, 633 (2005).
[4] A. M. Akulshin, S. Barreiro, and A. Lezama, Phys. Rev.

- A **57**, 2996 (1998).
[5] E. Arimondo, Progress in Optics **35**, 257 (1996).
[6] A. V. Taichenachev, A. M. Tumaikin, and V. I. Yudin, Phys. Rev. A **61**, 011802(R) (1999).
[7] G. Goren, A. D. Wilson-Gordon, M. Rosenbluh, and H. Friedmann, Phys. Rev. A **69**, 053818 (2004).

- [8] T. Zigdon, A. D. Wilson-Gordon, C. Goren, M. Rosenbluh, and H. Friedmann, SPIE Conference Proceedings **6604**, 660402 (2007).
- [9] C. Goren, A. D. Wilson-Gordon, M. Rosenbluh, and H. Friedmann, Phys. Rev. A **67**, 033807 (2003).
- [10] R. Meshulam, T. Zigdon, A. D. Wilson-Gordon, and H. Friedmann, Opt. Lett. **32**, 2318 (2007).
- [11] T. Zigdon, A. D. Wilson-Gordon, and H. Friedmann, Phys. Rev. A **77**, 033836 (2008).
- [12] C. Goren, A. D. Wilson-Gordon, M. Rosenbluh, and H. Friedmann, Phys. Rev. A **70**, 043814 (2004).
- [13] S. Singh and G. S. Agarwal, J. Opt. Soc. Am. B **5**, 2515 (1988).
- [14] A. D. May, Phys. Rev. A **59**, 3495 (1999).
- [15] H. Failache, P. Valente, G. Ban, V. Lorent, and A. Lezama, Phys. Rev. A **67**, 043810 (2003).
- [16] C. Bolkart, D. Rostohar, and M. Weitz, Phys. Rev. A **71**, 043816 (2005).
- [17] M. Shuker, O. Firstenberg, A. Ben-Kish, A. Ron, and N. Davidson, Phys. Rev. A **76**, 023813 (2007).
- [18] O. Firstenberg, M. Shuker, A. Ben-Kish, D. R. Fredkin, N. Davidson, and A. Ron, Phys. Rev. A **76**, 023813 (2007).
- [19] O. Firstenberg, M. Shuker, R. Pugatch, D. R. Fredkin, N. Davidson, and A. Ron, Phys. Rev. A **77**, 043830 (2008).
- [20] Y. Xiao, I. Novikova, D. F. Phillips, and R. Walsworth, Phys. Rev. Lett. **96**, 043601 (2006).
- [21] Y. Xiao, I. Novikova, D. F. Phillips, and R. L. Walsworth, Opt. Express **16**, 14128 (2008).
- [22] S. G. Rautian and I. I. Sobel'man, Sov. Phys. USPEKHI **9**, 701 (1967).
- [23] A. Lezama, S. Barreiro, and A. M. Akulshin, Phys. Rev. A **59**, 4732 (1999).
- [24] M. Shuker, O. Firstenberg, R. Pugatch, A. Ron, and N. Davidson, Phys. Rev. Lett. **100**, 223601 (2008).
- [25] O. Firstenberg, P. London, M. Shuker, A. Ron, and N. Davidson, Nature Physics **5**, 665 (2009).
- [26] The fact that the 'inner' decoherence rate γ is shared by both the ground and the excited manifolds, does not imply that their total decoherence rate is the same; the coherence between the two excited states decays via the $e \rightarrow g$ relaxation channels and therefore decays much faster than the ground-state coherence. Incorporating different values of γ for the ground and excited states does not lead to substantial changes in the collision-induced phenomena explored here.
- [27] When $\gamma_{\text{vcc}} \rightarrow 0$, the third term in Eq. (7) gradually vanishes, and the second term ($V_2^2 G_5$) is responsible for the EIA peak, as indicated by the brown-dotted line in Fig. 2(b). Its width is limited by homogenous broadening mechanisms and determined by γ and Γ_{pcc} .